Continuous Measurement of a Microwave-Driven Solid State Qubit

S. D. Barrett[1,*] and T. M. Stace[2,†]

[1]*Hewlett-Packard Laboratories, Filton Road, Stoke Gifford, Bristol BS34 8QZ, United Kingdom*
[2]*DAMTP, University of Cambridge, Wilberforce Road, CB3 0WA, United Kingdom*

(Received 9 December 2004; published 13 January 2006)

We analyze the dynamics of a continuously observed, damped, microwave-driven solid state charge qubit, consisting of a single electron in a double well potential. The microwave field induces transitions between the qubit eigenstates, which have a profound effect on the detector output current. Useful information about the qubit dynamics, such as dephasing and relaxation rates, and the Rabi frequency, can be extracted from the detector conductance and output noise power spectrum. We also propose a technique for single-shot electron *spin* readout, for spin based quantum information processing, which has a number of practical advantages over existing schemes.

DOI: 10.1103/PhysRevLett.96.017405 PACS numbers: 78.70.Gq, 03.67.Lx, 42.50.Lc, 63.20.Kr

Recent progress in mesoscopic physics has meant that it is now possible to confine, manipulate, and measure small numbers of electrons in single or coupled quantum dots [1–4]. These experiments are particularly interesting as they allow the complex interaction between such confined systems and their environment to be studied at the single electron level. In view of the potential applications of such systems in solid state quantum information processing (QIP) [5], understanding these interactions is important for characterizing decoherence.

Of particular interest are coupled quantum dot (CQD) qubit systems driven by oscillating electric fields. The presence of a driving field resonant to the qubit energy splitting drives transitions into the excited state. Continuous measurement of such systems can reveal important spectroscopic information about the qubit, such as the qubit splitting, Rabi frequency, and decoherence rates. Earlier work focussing on current transport *through* open CQD systems [6–8] has shown that this information can be extracted from the current and shot noise. In a recent experiment, a driven qubit comprising a single electron in a closed CQD system was *noninvasively* observed via a nearby quantum point contact (QPC) detector [4]. This noninvasive approach has several advantages over transport measurements. It allows access to the charging regime where only a single electron resides in the CQD. Further, in a transport measurement, an upper limit on the qubit decoherence time is set by the time scale for tunneling through the CQD, which must be sufficiently short for a measurable current to be detected.

In this Letter, we theoretically analyze this system (see Fig. 1). We account for the coupling of the CQD both to the QPC and to a generic bosonic environment [9], both of which contribute to the qubit relaxation and dephasing. Our results are also relevant to other driven qubit systems, e.g., superconducting charge qubits [10,11]. We also propose a method for spin readout, which offers improvements over existing schemes [3,12–14].

Previous works have considered the continuous measurement of *undriven* charge qubit systems by a QPC detector [15–17] and of driven superconducting flux qubits [18]. Here, we adopt the quantum trajectories description of the measurement process [16,17,19], and generalize results obtained in previous work [20,21] on the measurement of *undriven* charge qubits using a QPC at arbitrary bias voltage. We derive a master equation (ME) for the qubit and use this to determine the dc conductance and current power spectra of the QPC detector, and show how various qubit parameters can be extracted from these quantities. We then describe our technique for spin readout.

The model system we consider (Fig. 1) has total Hamiltonian $H = H_{\rm sys} + H_{\rm drive} + H_{\rm meas} + H_{\rm leads} + H_{\rm sb} + H_{\rm env}$, where ($\hbar = 1$)

$$H_{\rm sys} = (-\Delta\sigma_x - \epsilon\sigma_z)/2 \equiv -\phi\sigma_z^{(e)}/2, \tag{1}$$

$$H_{\rm drive} = \Omega_0 \cos[(\phi - \eta)t](\cos\delta\sigma_z + \sin\delta\sigma_x), \tag{2}$$

$$H_{\rm meas} = \sum_{k,q} \lambda(\mathcal{T} + \nu\sigma_z) a_{D,q}^\dagger a_{S,k} + \text{H.c.}, \tag{3}$$

$$H_{\rm leads} = \sum_k \omega_{S,k} a_{S,k}^\dagger a_{S,k} + \sum_q \omega_{D,q} a_{D,q}^\dagger a_{D,q}, \tag{4}$$

$$H_{\rm sb} = \sigma_z \sum_i \kappa_i (b_i^\dagger + b_i), \quad H_{\rm env} = \sum_i \omega_{B,i} b_i^\dagger b_i. \tag{5}$$

Here, $H_{\rm sys}$ is the bare qubit Hamiltonian, in which $\sigma_x = |l\rangle\langle r| + |r\rangle\langle l|$ and $\sigma_z = |l\rangle\langle l| - |r\rangle\langle r|$, where $|l\rangle$ ($|r\rangle$) denotes an electron state localized on the left (right) dot, $\phi = \sqrt{\Delta^2 + \epsilon^2}$ is the qubit energy splitting, and $\sigma_z^{(e)} = |g\rangle\langle g| - |e\rangle\langle e|$, where $|g\rangle = \cos\frac{\theta}{2}|l\rangle + \sin\frac{\theta}{2}|r\rangle$ and

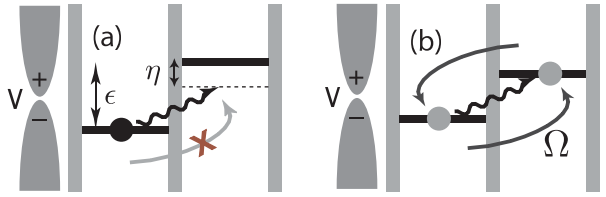

FIG. 1 (color online). Schematic of a CQD measured by a QPC under (a) nonresonant and (b) resonant driving.

$|e\rangle = \cos\frac{\theta}{2}|r\rangle - \sin\frac{\theta}{2}|l\rangle$ are the eigenstates of $H_{\rm sys}$, with $\tan\theta = \Delta/\epsilon$. $H_{\rm drive}$ corresponds to the driving field with frequency $\omega_0 = \phi - \eta$, which may couple to both the σ_x and σ_z qubit operators, as parametrized by δ. $H_{\rm meas}$ denotes the qubit-detector coupling, in terms of the dimensionless tunneling parameters $\mathcal{T} = \sqrt{2\pi g_S g_D}T$ and $\nu = \sqrt{2\pi g_S g_D}\chi$, and $\lambda = 1/\sqrt{2\pi g_S g_D}$. We have assumed that the tunneling amplitudes, T and χ, and the densities of lead modes, g_S and g_D, are approximately independent of k and q over the energy range where tunneling is allowed. $H_{\rm leads}$ is the free Hamiltonian of the source and drain leads, where $a_{S,j}$ ($a_{D,j}$) is the annihilation operator for an electron in the jth source (drain) mode. $H_{\rm sb}$ and $H_{\rm env}$ correspond to a standard spin-boson coupling to a generic bath of bosons [22], where b_i is the annihilation operator for the ith boson mode. We have neglected any qubit-bath coupling in $\sigma_{x,y}$, which typically scale with $\langle l|r\rangle$, so are negligible in the regime of interest [22].

We now derive a ME for the evolution of the qubit density matrix, ρ, as follows. First, to eliminate the time dependence from $H_{\rm sys} + H_{\rm drive}$, we transform to an interaction picture and make our first rotating wave approximation (RWA), neglecting terms oscillating rapidly compared to a Ω_0 and the microwave detuning, η. Next, to describe the qubit-QPC and qubit-environment interaction by Lindblad terms, we transform to a frame in which all the dynamics is contained in the qubit-QPC and qubit-environment terms, then make the Born-Markov approximation and a second RWA. Transforming back to the original interaction picture gives a Lindblad ME with time independent coefficients, as required.

In more detail, the first RWA is performed by transferring to an interaction picture defined by $H_0 = -\omega_0\sigma_z^{(e)}/2 + H_{\rm leads} + H_{\rm env}$, and neglecting rapidly oscillating terms in the transformed driving Hamiltonian. This is valid provided $\Omega_0 \ll \omega_0$. The Hamiltonian becomes

$$H_I(t) = -\frac{\Omega}{2}\sigma_x^{(e)} - \frac{\eta}{2}\sigma_z^{(e)} + A_I(t)Y(t) + B_I(t)Z(t), \quad (6)$$

where $\Omega = \Omega_0\sin(\theta - \delta)$, and $\sigma_x^{(e)} = |e\rangle\langle g| + |g\rangle\langle e|$. The operators $A_I(t) = e^{iH_0t}(\mathcal{T} + \nu\sigma_z)e^{-iH_0t}$ and $B_I(t) = e^{iH_0t}\sigma_z e^{-iH_0t}$ act on the system, and $Y(t) = \lambda\sum_{k,q}(e^{-i(\omega_{S,k}-\omega_{D,q})t}a_{D,q}^\dagger a_{S,k} + \text{H.c.})$ and $Z(t) = \sum_i\kappa_i(e^{-i\omega_{B,i}t}b_i^\dagger + \text{H.c.})$ act on the QPC and bosonic environment degrees of freedom, respectively.

To derive the ME for the dynamics of the qubit alone, we further transform to a frame defined by $H_0' = -\frac{\eta}{2}\sigma_z^{(e)} - \frac{\Omega}{2}\sigma_x^{(e)}$, giving a Hamiltonian $H_{I'}(t) = A_{I'}(t)Y(t) + B_{I'}(t)Z(t)$, where $A_{I'}(t)$ and $B_{I'}(t)$ are the transformed operators $A_I(t)$ and $B_I(t)$ of Eq. (6). These operators have several terms containing phase factors $e^{i\omega_n t}$, with frequencies $\omega_n = 0, \pm\Omega', \pm\omega_0, \pm\omega_0 \pm \Omega'$, where $\Omega' = \sqrt{\Omega^2 + \eta^2}$. The qubit density matrix satisfies [19]

$$\dot\rho_{I'}(t) = -\mathrm{Tr}_{S,D,B}\left\{\int_{t_0}^{t} dt'[H_{I'}(t),[H_{I'}(t'),R(t')]]\right\}, \quad (7)$$

where $R(t')$ is the total density matrix for the qubit, leads, and environment. We now make a Born-Markov approximation, setting $t_0 \to -\infty$ and $R(t') = \rho_{I'}(t)\otimes\rho_S\otimes\rho_D\otimes\rho_B$, where ρ_S, ρ_D, and ρ_B are equilibrium density matrices for the source, drain, and bath. This is valid provided the system-environment coupling is weak, and that $\rho_{I'}(t)$ changes slowly compared to the bath correlation times [19]. To describe the remaining approximations, we introduce the asymmetric quantum noise power spectra [23,24] for the QPC and bath, $S_Y(\omega) = \int_{-\infty}^{\infty}dt e^{i\omega t}\mathrm{Tr}[Y(t)Y(0)\rho_S\otimes\rho_D] = \Theta(\omega - eV) + \Theta(\omega + eV)$ and $S_Z(\omega) = \int_{-\infty}^{\infty}dt e^{i\omega t}\ \mathrm{Tr}\,[Z(t)Z(0)\rho_B] = 2\pi J(\omega)[1 + n(\omega)] + 2\pi J(-\omega)n(-\omega)$, where $\Theta(x) = (x + |x|)/2$, eV is the source-drain bias across the detector, $J(\omega) = \sum_i\kappa_i^2\delta(\omega - \omega_{B,i})$ is the bath spectral density, and $n(\omega)$ is the Bose occupation number. We now make a second RWA, where we neglect terms in Eq. (7) rotating at a rate ω_0, which is justified in the limit of weak coupling to the detector and environment, $\omega_0 \gg S_{Y,Z}(\omega_n)$ [25]. We also assume that the driving field is sufficiently weak that $S_{Y,Z}(\omega \pm \Omega') \approx S_{Y,Z}(\omega)$, i.e., that the noise spectra are slowly varying over frequencies of order Ω' [26]. Finally, in order to treat dephasing perturbatively, we require that, for small ω, $J(\omega) \propto \omega^s$ where $s \geq 1$.

These approximations allow us to derive a ME which is valid for arbitrary source-drain bias and bath temperature. Here, we restrict our attention to the low-bias ($eV < \phi$) and low-temperature ($kT \ll \phi$) regime, which has been probed in a recent experiment [4]. The ME in the original interaction picture is

$$\dot\rho_I(t) = -i\left[-\frac{\eta}{2}\sigma_z^{(e)} - \frac{\Omega}{2}\sigma_x^{(e)}, \rho_I(t)\right] + \frac{1}{2}\Gamma_\varphi\mathcal{D}[\sigma_z^{(e)}]\rho_I(t) + \Gamma_r\mathcal{D}[|g\rangle\langle e|]\rho_I(t), \quad (8)$$

where $\Gamma_\varphi = \Gamma_\varphi^{\rm det} + \Gamma_\varphi^{\rm env}$ is the pure dephasing rate, with $\Gamma_\varphi^{\rm det} = 2\nu^2\cos^2\theta S_Y(0)$ and $\Gamma_\varphi^{\rm env} = 2\cos^2\theta S_Z(0)$. $\Gamma_r = \Gamma_r^{\rm det} + \Gamma_r^{\rm env}$ is the relaxation rate, with $\Gamma_r^{\rm det} = \nu^2\cos^2\theta S_Y(\phi)$ and $\Gamma_r^{\rm env} = \cos^2\theta S_Z(\phi)$. We have also defined $\mathcal{D}[A]\rho = A\rho A^\dagger - (A^\dagger A\rho + \rho A^\dagger A)/2$.

dc conductance.—The dc current through the QPC is related to the steady state occupation probability of the dot nearest the QPC, to first order in ν, by $I = I_0 - \delta I\langle l|\rho(\infty)|l\rangle$, where $I_0 = (\mathcal{T}^2 - 2\nu\mathcal{T})eV$ corresponds to the current when the electron is localized in state $|r\rangle$, $\delta I = -4\nu\mathcal{T}eV$ [20,21], and $\rho(\infty)$ is the steady state of Eq. (8). The scaled conductance $[M = 1 + (I - I_0)/\delta I = 1 - \langle l|\rho(\infty)|l\rangle]$ is

$$M = \frac{1}{2} - \frac{\epsilon\Gamma_r(\eta^2 + \Gamma_{\varphi'}^2)}{2\phi[\eta^2\Gamma_r + \Gamma_{\varphi'}(\Omega^2 + \Gamma_r\Gamma_{\varphi'})]}, \quad (9)$$

where $\Gamma_{\varphi'} = \Gamma_\varphi + \Gamma_r/2$ is the total dephasing rate. M is

plotted as a function of ϵ in Fig. 2(a) and is in excellent qualitative agreement with recent experimental observations [4,10,11]. Note that these results are valid for weak driving, such that $\Omega_0 \ll \omega_0$. When $\Omega_0 \sim \omega_0$, qualitatively different effects are expected, such as, the appearance of multiphoton peaks [28]. Thus $\Omega_0 \ll \omega_0$ can be verified, e.g., by measuring the relative weight of the 1- and 2-photon peaks.

Useful spectroscopic information may be extracted from these resonant peaks at $\epsilon = \pm\sqrt{\omega_0^2 - \Delta^2}$. If the driving frequency, ω_0, is known, and the Rabi frequency, Ω, is known independently (e.g., from observations of the time dependence of the detector current, as discussed below) then Γ_r and $\Gamma_{\varphi'}$ can both be determined. When $\omega_0 \gg \Delta$ and assuming that Γ_r, $\Gamma_{\varphi'}$, and Ω do not vary significantly across the peak, from Eq. (9) we find $\Omega^2 \approx \Gamma_r\Gamma_{\varphi'}(\delta\epsilon^2/\Gamma_{\varphi'}^2 - 1)$, where $\delta\epsilon$ is the half width half maximum for the peak. Therefore, plotting Ω against $\delta\epsilon$ allows both Γ_r and $\Gamma_{\varphi'}$ to be determined. However, in the absence of time-resolved measurements, Ω may be unknown, because the relationship between the input microwave power and the electric field coupling to the qubit may be unknown. In this case, $\Gamma_{\varphi'}$ can still be extracted by plotting the peak height, h, against $\delta\epsilon$, for different values of the incident power. Again assuming $\omega_0 \gg \Delta$ and that Γ_r, $\Gamma_{\varphi'}$, and Ω do not vary significantly across the peak, h and $\delta\epsilon$ are related by $h \approx 1/2 - \Gamma_{\varphi'}^2/2\delta\epsilon^2$, which is independent of the (unknown) quantity Ω [see Fig. 2(b)]. For sufficiently weak driving, the peak width directly gives $\Gamma_{\varphi'}$, while for stronger driving, the peak width is proportional to Ω.

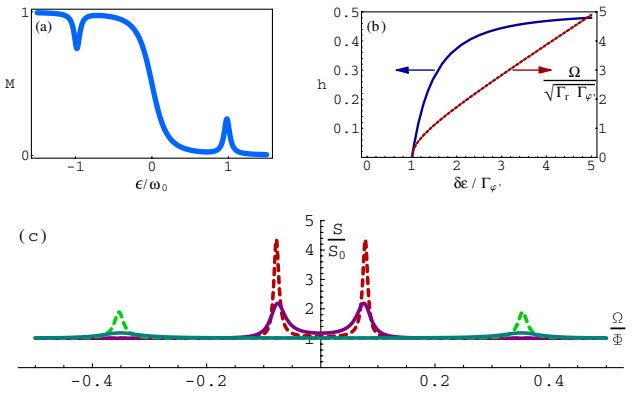

FIG. 2 (color online). (a) Variation in conductance (scaled between 0 and 1) vs dot bias. Parameters $\Gamma_\varphi = \Gamma_r = \Omega = 0.03\omega_0$ and $\Delta = 0.2\omega_0$ were taken to be constant over the entire range of ϵ. (b) The peak height h as a function of peak width $\delta\epsilon$. Increasing microwave power scans from left to right. Also shown is the relationship between $\delta\epsilon$ and the Rabi frequency Ω_0. (c) Power spectrum, $\tilde{S}(\omega)$. Inner peaks: $\theta = \pi/20$, outer peaks: $\theta = \pi/4$. The tall peaks have detector limited dephasing, $\Gamma_\varphi = \Gamma_\phi^{\rm det} = 2\nu^2 eV\cos^2\theta$, while the short peaks are dominated by phonon dephasing, $\Gamma_\varphi = 0.03/\phi$. Other parameters are $eV/\phi = 0.5$, $\nu = 0.1$, $\Omega_0/\phi = 0.5$.

Power spectrum.—Further spectroscopic information may be obtained from the power spectrum of the QPC current, which is given by $S(\omega) = 2\int_{-\infty}^{\infty} d\tau G(\tau)e^{-i\omega t}$, where $G(\tau) = E[I(t+\tau)I(t)] - E[I(t+\tau)]E[I(t)]$ is the current autocorrelation function, and $E[\ldots]$ denotes the classical expectation. $S(\omega)$ can be computed using the method in [17,21]. In the low-bias regime the scaled (symmetric) power spectrum $\tilde{S}(\omega) = S(\omega)/S_0$ (where $S_0 = 2eI \approx 2e^2\mathcal{T}^2V$ is the shot noise background) is closely approximated by

$$\tilde{S}(\omega) = \frac{s_{\Omega'}\gamma_{\Omega'}^2}{\gamma_{\Omega'}^2 + (\omega - \Omega')^2} + \frac{s_{\Omega'}\gamma_{\Omega'}^2}{\gamma_{\Omega'}^2 + (\omega + \Omega')^2} + \frac{s_0\gamma_0^2}{\gamma_0^2 + \omega^2} + 1, \tag{10}$$

where $\gamma_{\Omega'} = (2x\Gamma_\varphi + y\Gamma_r)/4z$, $\gamma_0 = (2\Omega^2\Gamma_\varphi + x\Gamma_r)/2z$, $s_{\Omega'} = 8\Omega^2\Gamma_\varphi^{\rm det}/(2x\Gamma_\varphi + y\Gamma_r)$, and $s_0 = 8\eta^2\Omega^2\Gamma_\varphi^{\rm det}(\Omega^2\Gamma_r^2 + 4x\Gamma_r\Gamma_\varphi + 4\Omega^2\Gamma_\varphi^2)/(2\Omega^2\Gamma_\varphi + x\Gamma_r)^3$, with $x = 2\eta^2 + \Omega^2$, $y = 2\eta^2 + 3\Omega^2$, and $z = \eta^2 + \Omega^2$.

The peak shapes and positions contain important information about the qubit. The height of the peaks at $\pm\Omega'$ is maximized when the external field is resonant with the qubit transition, $\eta = 0$. Note that $\tilde{S}(\Omega') \leq 5$ and thus the peak heights are no more than 4 times the shot noise background, as shown in Fig. 2(c). $\tilde{S}(\Omega') = 5$ only when dephasing is detector dominated.

Spin measurement.—Motivated by the preceding analysis, we propose a method for single-shot spin readout, using a microwave field and an inhomogeneous Zeeman splitting across the CQD. This splitting could be generated by an inhomogeneous magnetic or nuclear spin field, or engineering different g factors in each dot, such that $B_l \neq B_r$, where B_i denotes the Zeeman splitting on each site. In this case, one spin configuration, say spin-down, may be made resonant with the driving field, while the other, spin-up, is detuned by an amount η, and thus the spin can be determined by observing the current through the QPC [Fig. 3(a)]. Such a scheme is analogous to the method of spin readout via quantum jumps in atomic systems [29]. Alternative methods for spin readout have also been proposed [12–14,30,31].

The inhomogeneous Zeeman splitting amounts to a spin dependent bias between the dots, $\epsilon_{\downarrow/\uparrow} = \epsilon \pm (B_r - B_l)/2$. Thus the detector response is shifted for each spin configuration, as shown in Fig. 3(b). If $B_r - B_l \gtrsim \delta\epsilon$, the peaks are clearly resolved. If ϵ is tuned such that the spin-down transition is resonant with the driving field, the currents for each spin configuration are approximately $I_\uparrow \approx I_0 - \delta I$ and $I_\downarrow \approx I_0 - \delta I/2$. The shot noise limited time taken to resolve these currents is $\tau_{\uparrow\downarrow}^{-1} = (I_\uparrow^{1/2} - I_\downarrow^{1/2})^2/2e \approx \delta I^2/32I_0$. Thus $\tau_{\uparrow\downarrow} = 4\tau_{01}$ where τ_{01} is the time taken to distinguish the currents due to 0 and 1 electrons on dot "l." Shot noise limited QPC detection with $\tau_{01} \sim 25$ ns is possible [32], and so $\tau_{\uparrow\downarrow} \sim 100$ ns

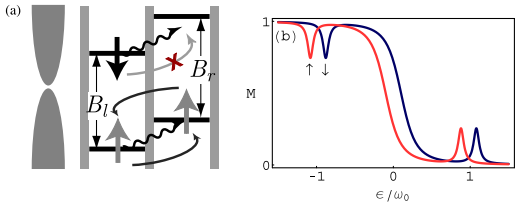

FIG. 3 (color online). (a) Schematic of spin measurement scheme. (b) Conductance curves for spin-up and spin-down configurations showing distinct resonance peaks.

should be achievable. This compares favorably with recently observed spin flip times ($T_1 \approx 1$ ms) in GaAs quantum dots [3], indicating that very high fidelity readout is possible.

The method offers some advantages over other schemes where no driving is used. First, a relatively small differential Zeeman splitting is needed, $B_r - B_l \gtrsim \delta\epsilon$. The peak width satisfies $\delta\epsilon \gtrsim \Gamma_{\varphi'}$, so for a charge dephasing rate of $\Gamma_{\varphi'} \sim 10^8$ s^{-1} [2], we require $B_r - B_l \gtrsim 0.07$ μeV. For readout via an inhomogenous Zeeman splitting but without driving [13], to obtain a comparable signal-to-noise, the differential Zeeman splitting must be larger than the central transition region in Fig. 3(b), i.e., $B_r - B_l \gtrsim \max(\Delta, kT)$. For $T = 100$ mK, $B_r - B_l \gtrsim 9$ μeV is required. Thus in GaAs ($g = 0.44$), with a uniform field of 1 T, our scheme requires a g-factor variation between the dots of $\Delta g/g \sim 0.3\%$, whereas without driving, one would require $\Delta g/g \sim 35\%$.

Second, by switching the microwave frequency first on resonance with the spin-down transition, and then on resonance with the spin-up transition, a definite signal is always obtained for both spin states. This is in contrast to other measurement schemes in which a definite signal is only registered for one spin configuration, [3,12–14], with the other state indicated only by the lack of a signal.

In summary, we have analyzed the dynamics of a continuously observed, damped, driven solid state qubit. The dephasing rate $\Gamma_{\varphi'}$, can be extracted from dc measurements of the QPC current alone, even when the coupling between the microwave field and the qubit is unknown. If the power spectrum of the QPC output noise can be measured, then the relaxation rate Γ_r and Rabi frequency Ω can also be determined. We have also proposed a single-shot spin readout technique using microwave driving, which offers advantages over existing schemes and can be implemented with current technology.

We thank Gerard Milburn, Charles Smith, Andrew Doherty, Jason Petta, Charlie Marcus, Bill Munro, and Tim Spiller for useful conversations. S. D. B. thanks the EU NANOMAGIQC project for support. T. M. S. is funded by the CMI-Fujitsu Collaboration.

*Electronic address: seandbarrett@gmail.com

†Electronic address: tms29@cam.ac.uk

[1] R. Hanson *et al.*, Phys. Rev. Lett. **91**, 196802 (2003); J. M. Elzerman *et al.*, Phys. Rev. B **67**, 161308(R) (2003); S. Gardelis *et al.*, Phys. Rev. B **67**, 073302 (2003); A. W. Rushforth *et al.*, Phys. Rev. B **69**, 113309 (2004); L. DiCarlo *et al.*, Phys. Rev. Lett. **92**, 226801 (2004); T. Fujisawa *et al.*, Nature (London) **419**, 278 (2002).
[2] T. Hayashi *et al.*, Phys. Rev. Lett. **91**, 226804 (2003).
[3] J. M. Elzerman *et al.*, Nature (London) **430**, 431 (2004).
[4] J. R. Petta *et al.*, Phys. Rev. Lett. **93**, 186802 (2004).
[5] D. Loss and D. P. DiVincenzo, Phys. Rev. A **57**, 120 (1998).
[6] R. Aguado and T. Brandes, Phys. Rev. Lett. **92**, 206601 (2004).
[7] T. H. Oosterkamp *et al.*, Nature (London) **395**, 6705 (1998).
[8] T. Brandes, R. Aguado, and G. Platero, Phys. Rev. B **69**, 205326 (2004).
[9] S. D. Barrett and G. J. Milburn, Phys. Rev. B **68**, 155307 (2003).
[10] K. W. Lehnert *et al.*, Phys. Rev. Lett. **90**, 027002 (2003).
[11] T. Duty *et al.*, Phys. Rev. B **69**, 140503(R) (2004).
[12] T. M. Stace *et al.*, Phys. Rev. B **70**, 205342 (2004).
[13] H.-A. Engel *et al.*, Phys. Rev. Lett. **93**, 106804 (2004).
[14] S. D. Barrett and T. M. Stace, cond-mat/0411581.
[15] A. N. Korotkov, Phys. Rev. B **60**, 5737 (1999); A. N. Korotkov and D. V. Averin, Phys. Rev. B **64**, 165310 (2001); S. A. Gurvitz, Phys. Rev. B **56**, 15 215 (1997); S. A. Gurvitz *et al.*, Phys. Rev. Lett. **91**, 066801 (2003); Y. Makhlin, G. Schön, and A. Shnirman, Phys. Rev. Lett. **85**, 4578 (2000); S. Pilgram and M. Büttiker, Phys. Rev. Lett. **89**, 200401 (2002).
[16] H.-S. Goan *et al.*, Phys. Rev. B **63**, 125326 (2001).
[17] H.-S. Goan and G. J. Milburn, Phys. Rev. B **64**, 235307 (2001).
[18] A. Y. Smirnov, Phys. Rev. B **68**, 134514 (2003).
[19] C. W. Gardiner and P. Zoller, *Quantum Noise* (Springer, New York, 2000).
[20] T. M. Stace and S. D. Barrett, Phys. Rev. Lett. **92**, 136802 (2004).
[21] T. M. Stace and S. D. Barrett, cond-mat/0309610.
[22] A. J. Leggett *et al.*, Rev. Mod. Phys. **59**, 1 (1987).
[23] R. Aguado and L. P. Kouwenhoven, Phys. Rev. Lett. **84**, 1986 (2000).
[24] R. J. Schoelkopf *et al.*, cond-mat/0210247.
[25] This RWA implies a course graining in time, which means that our treatment does not describe dynamics on very short time scales of order ϕ^{-1}.
[26] For strong driving, the approximation $S_{Y,Z}(\omega \pm \Omega') \approx S_{Y,Z}(\omega)$ breaks down, and a *population inversion* can occur [27].
[27] T. M. Stace, A. C. Doherty, and S. D. Barrett, Phys. Rev. Lett. **95**, 106801 (2005).
[28] C. A. Stafford and N. S. Wingreen, Phys. Rev. Lett. **76**, 1916 (1996).
[29] R. Blatt and P. Zoller, Eur. J. Phys. **9**, 250 (1988).
[30] M. Friesen *et al.*, Phys. Rev. Lett. **92**, 037901 (2004).
[31] L. C. L. Hollenberg *et al.*, Phys. Rev. B **69**, 233301 (2004).
[32] L. M. K. Vandersypen *et al.*, Appl. Phys. Lett. **85**, 4394 (2004).